

Fully frustrated XY model with next-nearest-neighbor interaction

Giancarlo Franzese,^{1,2,3,*} Vittorio Cataudella,^{1,2} S. E. Korshunov,⁴ and Rosario Fazio^{1,5}

¹*Istituto Nazionale per la Fisica della Materia (INFM), Unità di Napoli e Catania, Italy*

²*Dipartimento di Scienze Fisiche, Università "Federico II," Mostra d'Oltremare, Padiglione 19, 80125 Napoli, Italy*

³*Dipartimento di Fisica "E. Amaldi," Università Roma Tre, via della Vasca Navale 84, 00146 Roma, Italy*

⁴*L. D. Landau Institute for Theoretical Physics, Kosygina 2, 117940 Moscow, Russia*

⁵*Dipartimento di Metodologie Fisiche e Chimiche (DMCFI), Università di Catania, viale A. Doria 6, 95125 Catania, Italy*

(Received 24 July 2000)

We investigate a fully frustrated XY model with nearest-neighbor (NN) and next-nearest-neighbor (NNN) couplings which can be realized in Josephson junction arrays. We study the phase diagram for $0 \leq x \leq 1$ (x is the ratio between NNN and NN couplings). When $x < 1/\sqrt{2}$ an Ising transition and a Berezinskii-Kosterlitz-Thouless transition are present. Both critical temperatures decrease with increasing x . For $x > 1/\sqrt{2}$ the array undergoes a sequence of two transitions. On raising the temperature first the two sublattices decouple from each other and then, at higher temperatures, each sublattice becomes disordered. The structure of phase diagram remains the same if weak interaction with further neighbors is included.

A variety of two-dimensional systems undergo a phase transition without a rigorous symmetry breaking, the Berezinskii-Kosterlitz-Thouless (BKT) transition.¹ The transition is driven by the thermally excited vortices which form a two-dimensional Coulomb gas.² Josephson-junction arrays are experimental realization of the two-dimensional XY model where the array's parameters can be modified in a controlled way. In the last decade there has been a great amount of work on the various aspects of the BKT transition in Josephson arrays.³ Experimental studies are based on electrical resistance,⁴ two-coil inductance,⁵ and superconducting quantum interference device⁶ measurements.

A magnetic field applied perpendicularly to the array leads to frustration.^{7,8} If the flux piercing the elementary plaquette is half of the flux quantum $\Phi_0 = hc/2e$, the system is called fully frustrated (FF) and undergoes two phase transitions related to the Z_2 and $U(1)$ symmetries. The existence of the two critical temperatures $T_c^{Z_2}$ and $T_c^{U(1)}$, respectively has been extensively investigated both by analytical methods^{8,9} and Monte Carlo (MC) simulations.¹⁰⁻¹⁴ The complete scenario is not fully understood yet. There are numerical evidences either supporting the existence of two very close critical temperatures ($T_c^{Z_2} > T_c^{U(1)}$) with critical behavior typical of Ising and BKT transitions, respectively,¹³⁻¹⁵ or the existence of a single transition with unusual critical behavior.¹¹

In this paper we study the properties of a two-dimensional FF Josephson array with both nearest-neighbor (NN) and next-to-nearest neighbor (NNN) couplings.^{16,17} The analogous system with unfrustrated NN interaction has been considered by Henley.¹⁸ Proximity-junction arrays may be good candidates to experimentally probe the effects discussed in this work. They consist of superconducting islands in good electric contact with a metallic substrate. Due to the proximity effect there is a leakage of Cooper pairs into the normal substrate which extends over a temperature-dependent coherence length ξ_N ($\xi_N = \hbar v_F / k_B T$ or $\xi_N = \sqrt{\hbar D / 2\pi k_B T}$ for the ballistic and for the diffusive case, respectively, v_F is the

Fermi velocity, D the diffusion constant, and T the temperature). When ξ_N becomes comparable with the lattice constant of the array the NNN coupling becomes comparable with the NN coupling. Since ξ_N is strongly dependent on the temperature, the NNN Josephson coupling may be observed cooling down the sample. The main results of this paper are summarized in the phase diagram of Fig. 5.

The system is defined by the Hamiltonian

$$H = - \sum_{\langle\langle i,j \rangle\rangle} J_{ij} \cos(\theta_i - \theta_j - A_{ij}), \quad (1)$$

where $J_{ij} = J > 0$ for NN and $J_{ij} = xJ$ for NNN ($x \geq 0$), the symbol $\langle\langle \dots \rangle\rangle$ refers to the sum over NN and NNN. Here we treat them as independent coupling. In the experimental situation the ratio of the couplings changes with temperature in accordance with temperature dependence of the coherence length

For later convenience we introduce the gauge invariant phase difference $\phi_{ij} = \theta_i - \theta_j - A_{ij}$. The variables θ_i are the phases of the superconducting order parameter of the i th island. The magnetic field enters through $A_{ij} = (2\pi/\Phi_0) \int_i^j \mathbf{A} \cdot d\mathbf{l}$ (\mathbf{A} is the vector potential). The relevant parameter which describes the magnetic frustration is $f = \sum A_{ij} / (2\pi)$, where the summation runs over the perimeter of the elementary plaquette. We study the case $f = 1/2$ on a square lattice.

Ground states. The model of Eq. (1) combines the characteristics of both the FF and unfrustrated XY models. While the elementary square plaquette is FF, the value of the magnetic flux for the square plaquettes formed by NNN couplings is equal to Φ_0 and therefore NNN interaction (considered by itself) is not frustrated. For $x < x_0 \equiv 1/\sqrt{2}$ we find that the ground state of this system is exactly the same as in the FF model without NNN couplings and is characterized by $\phi_{ij} = \pm \pi/4$ for all pairs of NN sites. This state combines continuous [$U(1)$] and discrete (Z_2) degeneracies. Its energy per site $E = -\sqrt{2}J$ is independent of NNN coupling xJ . Moreover if one considers a straight domain wall separating

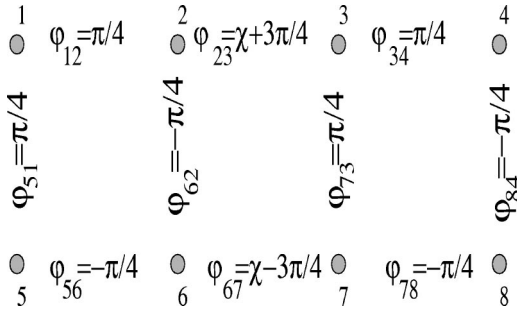


FIG. 1. The family of the additional (intermediate) ground states at the degeneracy point $x=1/\sqrt{2}$ is characterized by the angle χ . The value $\chi=\pi$ corresponds to the low- x ground state while $\chi=0$ corresponds to the high- x ground state with a particular relative phase shift between the two sublattices. The angle reported in the figure is the gauge invariant phase difference between two neighboring sites.

the two ground states with opposite orientations of chiralities it turns out that neither the form of such state nor its energy change with addition of NNN interactions.

For $x>x_0$ the ground state is the same as in the absence of NN coupling when the system splits into two unfrustrated XY models. The relative phase shift between the two sublattices can be arbitrary. The energy of this state $E=-2xJ$ depends only on NNN coupling xJ and does not depend on NN coupling.

At the special point $x=x_0$ the energies of both the above ground states coincide. Moreover they can be transformed into each other by a continuous transformation without increasing the energy of the system. Therefore the manifold of the ground states also includes an additional set of eight-sublattice ‘‘intermediate’’ states which can be parametrized by a rotation angle χ ($\chi=\pi$ corresponding to low- x ground state and $\chi=0$ corresponding to high- x ground state with a particular relative phase shift between the sublattices) as is shown in Fig. 1.

Quite remarkably the inclusion of weak interaction with further neighbors (at least those of the third and the fourth order) does not lead to any qualitative changes, but only to the shift of x_0 . In particular, all the ground states remain the same and for $x>x_0$ the energy remains independent of the phase shift between the sublattices.

Phase diagram. We studied the finite-temperature behavior of the model by means of the (low-temperature) spin-wave free energy analysis and by Monte Carlo simulations.

For $x<x_0$ neither the spectrum of spin waves (in the long-wavelength limit) nor the domain wall energy depend on x . Therefore we can expect only a weak dependence of $T_c^{Z_2}$ and $T_c^{U(1)}$ on x , due to the change of the effective interaction between the different types of fluctuations.

For $x>x_0$ the system (at finite temperatures) turns out to be equivalent to two coupled XY models, the effective coupling between the two sublattices of the form $\cos 4(\theta-\theta')$ provided by the free energy of small amplitude order parameter fluctuations (spin waves). Although this coupling is weak (always much smaller than the temperature) at low temperatures it is relevant and imposes the presence of a transition at the temperature $T=T_D$ for which both sublattices in absence of coupling would be in the quasicrystallized

state.^{19,20} This transition separates the phases with coupled and decoupled sublattices and is related with an additional breaking of a discrete symmetry group. In the low-temperature phase, where the two sublattices are locked, the spin-wave contribution to the free energy imposes a relative phase shift of $\pm\pi/4$ (or equivalently $\pm 3\pi/4$) between the two sublattices. At $T>T_D$ a second phase transition of the BKT type takes place in each of the decoupled sublattices. For $x\gg x_0$ the temperature of this transition depends only on NNN coupling and it is proportional to x .

The spin-wave spectrum remains rigid down to $x=x_0$. This indicates (and it is confirmed by the MC simulations) that the critical temperature of this BKT transition remains finite when $x\rightarrow x_0^+$. Below this temperature there is a transition between the FF low- x and the unfrustrated high- x phases. We evaluated numerically the spin-wave free energy of the intermediate ground state as a function of χ . This dependence is described by a convex function implying a first-order phase transition line separating the low- x and high- x quasicrystallized phases.

The critical properties were investigated evaluating the staggered chiral magnetization M and the helicity modulus Γ by means of standard MC simulations for different x . The order parameter M , which controls the Ising-like transition, is defined as

$$M = \frac{1}{L^2} \left| \sum_i (-1)^{i_x+i_y} m_i \right|, \quad (2)$$

where $\vec{r}_i/a=(i_x, i_y)$ is the position vector (in unit of lattice step a) of the site i and $m_i=(1/\sqrt{8})(\sin\phi_{i,j_1} + \sin\phi_{j_1,j_2} + \sin\phi_{j_2,j_3} + \sin\phi_{j_3,i})$ is the chirality of the plaquette with center in $(i_x+1/2, i_y+1/2)$ and with site indexes i, j_1, j_2, j_3 (in clockwise order).

In order to obtain a precise determination of $T_c^{Z_2}$ and of the critical exponent ν associated to the divergence of the correlation length we have calculated the Binder’s cumulant²¹ of the staggered chiral magnetization M

$$U_M = 1 - \frac{\langle M^4 \rangle}{3\langle M^2 \rangle^2}. \quad (3)$$

Since $U_M(T_c^{Z_2}, L)$ does not depend on lattice size L for large systems, $T_c^{Z_2}$ can be identified without making any assumption on the critical exponents. Once a satisfactory estimation of $T_c^{Z_2}$ is obtained the critical exponent ν is estimated through a data collapsing with ν left as the only free parameter. Estimations of U_M have been obtained averaging, at least, $10^7 L^2$ MC configurations by using a standard Metropolis algorithm. The largest lattice studied is $L=72$. The results for $x=0.5$ are shown in Figs. 2 and 3(a). We estimate $k_B T_c^{Z_2}/J=0.403\pm 0.003$. The data collapsing, shown in the inset of Fig. 2, give an estimate of $1/\nu=1.0\pm 0.1$. The critical temperature $T_c^{Z_2}$ decreases with increasing x for $x<x_0$. For $x\geq x_0$, there is no sign of a Ising-like transition [see Fig. 3(b)].

The helicity modulus $\Gamma = \partial^2 \mathcal{F} / \partial \delta^2$, used to signal the existence of a BKT transition, is defined through the increase of the free energy \mathcal{F} due to a phase twist δ imposed in one

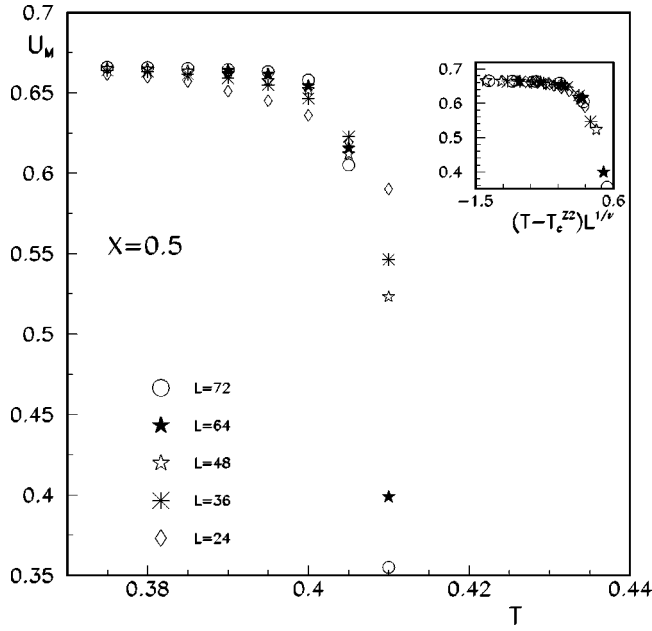


FIG. 2. The Binder's parameter U_M vs T for several lattice sizes L at $x=0.5$. Errors are smaller than the symbol size. Excluding the data of smallest size ($L=24$) one can estimate $0.400 < k_B T_c^{Z2}/J < 0.406$. Inset: Collapse of the data (excluding the $L=24$ points). The scaling parameters are $k_B T_c^{Z2}/J = 0.403 \pm 0.003$ and $1/\nu = 1.0 \pm 0.1$.

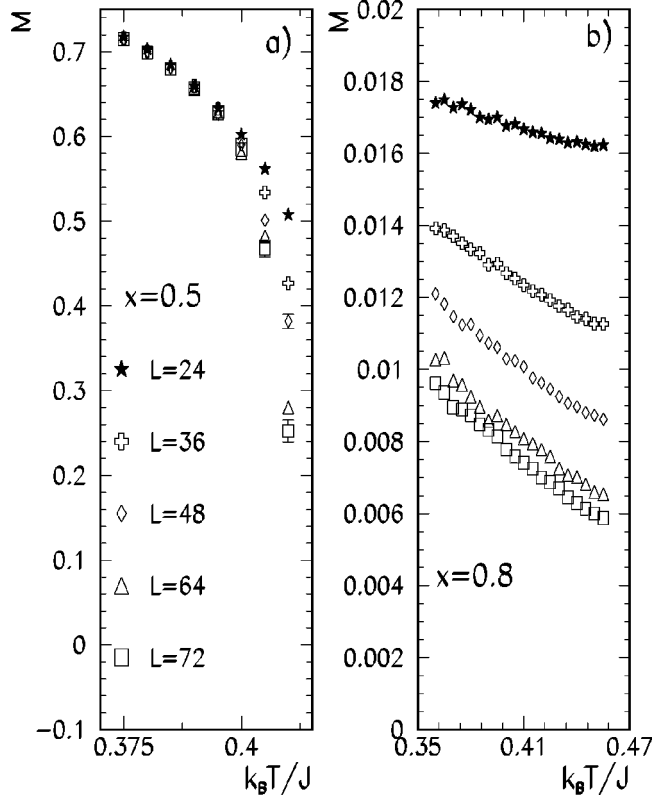


FIG. 3. The staggered chiral magnetization M vs T for $x=0.5$ (a) and $x=0.8$ (b). For large L and low T , M goes to a nonzero value for $x=0.5$ and vanishes for $x=0.8$. The errors are smaller than the symbol size. The symbols for different lattice sizes are the same in (a) and (b).

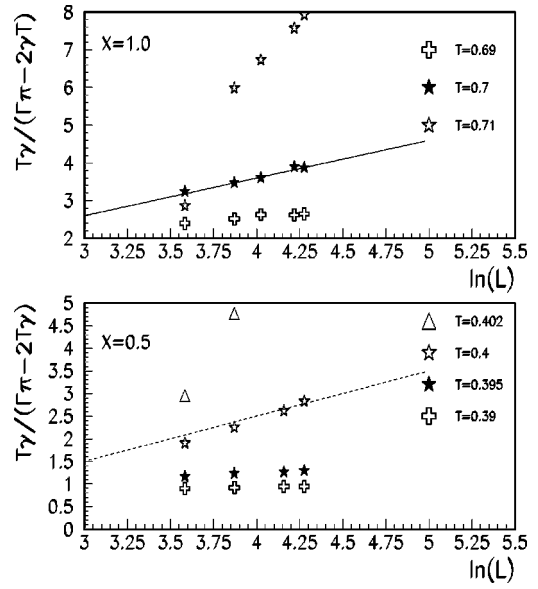


FIG. 4. The size dependence of the helicity modulus Γ for $x=0.5$ and $x=1$ at several temperatures T . The errors are smaller than the symbol size. The form of the plot $[\gamma T/(\pi\Gamma - 2\gamma T)]$ vs $\ln L$ is chosen in such a way that the scaling behavior predicted by Eq. (4) should correspond to a straight line with the slope equal to 1 (as shown by the overimposed lines). The estimates for the critical temperature $T_c^{U(1)}$ are 0.4 and 0.7, respectively. The error on the estimates is due to the used temperature mesh.

direction.²² Following the procedure proposed in Refs. 23 and 24, the critical temperature $T_c^{U(1)}$ is estimated by using the following *ansatz* for the size dependence of Γ :

$$\frac{\pi\Gamma}{2T_c} = \gamma \left[1 + \frac{1}{2(\ln L - \ln l_0)} \right], \quad (4)$$

where l_0 is a fit parameter. This critical scaling is based on the mapping between a neutral Coulomb gas and an XY model. Therefore Eq. (4) can be used both as a test for the existence of a BKT transition and for a precise evaluation of the critical temperature. A very good scaling was obtained with $\gamma=1$ (the ordinary BKT transition) in the low- x phase and $\gamma=2$ (corresponding to the BKT transition on each of the two sublattices with lattice constant $\sqrt{2}$) in the high- x phase. In Fig. 4 we show this analysis for the cases $x=0.5$ and $x=1$. $T_c^{U(1)}(x)$, as well as $T_c^{Z2}(x)$, decreases with increasing x up to $x \sim x_0$. Our results cannot discriminate between the $T_c^{Z2} = T_c^{U(1)}$ and the $T_c^{Z2} > T_c^{U(1)}$ hypothesis since the two temperatures are compatible within the numerical precision [the mean value of $T_c^{Z2}(x)$ remains always above the corresponding mean value of $T_c^{U(1)}(x)$]. For $x \geq 0.8$, instead, $T_c^{U(1)}(x)$ increases, quickly tending towards the value expected for $x \rightarrow \infty$, i.e., $k_B T_c^{U(1)}/(xJ) = 0.89$.

We finally discuss the transition related to the decoupling of sublattices in the high- x phase. The order parameter $S = \sum_{j,\alpha} s_{j,j+e_\alpha}$ can be defined on the bonds of the lattice and can be chosen in the following gauge-invariant form:

$$s_{j,j+e_x} = (-1)^{j_x} \exp[i(-1)^{j_x+j_y} \phi_{j,j+e_x}],$$

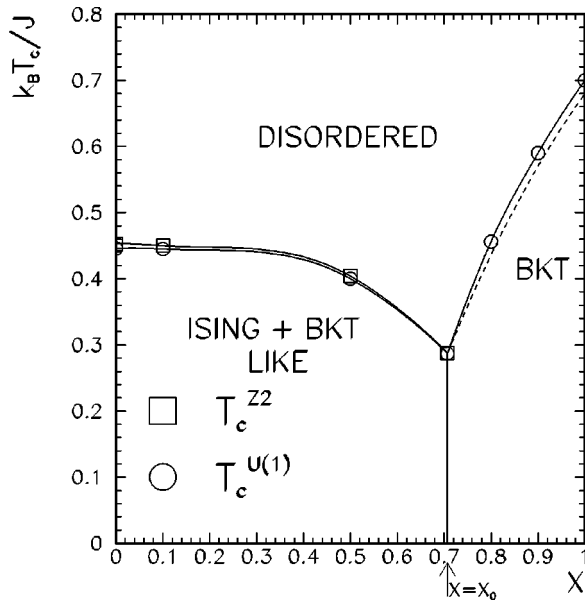


FIG. 5. The phase diagram for the XY model with NN+NNN interactions. Squares refer to $T_c^{Z_2}$, circles to $T_c^{U(1)}$; x is the ratio between NNN and NN couplings; J is the NN coupling. The errors are smaller than the symbol size (see text for details). The dotted line shows the qualitative behavior of the transition associated to the decoupling of the two NNN sublattices.

$$s_{j,j+e_y} = i(-1)^{j_y} \exp[i(-1)^{j_x+j_y} \phi_{j,j+e_y}].$$

This form of the order parameter is chosen in such way that for any of the high- x ground states the value of s will be the same for all the bonds. At low temperatures S manifests a true long-range order. The MC simulations confirm the $\pi/4$ relative phase shift anticipated by the spin-wave analysis. By

increasing the temperature the long-range order in S can be expected to disappear as a separate phase transition whereas the unbinding of vortex pairs in each of the sublattices has to occur at still higher temperatures. We performed MC simulations to evaluate the transition temperature T_D . The preliminary results of this computation (not reported here) indicate that T_D is very close, but lower, than the transition to the disordered phase $T_c^{U(1)}(x)$. More extensive simulations are needed to determine the critical behavior of the decoupling transition. The dotted line in Fig. 5 shows qualitatively the expected behavior of the decoupling transition temperature as a function of x .

In conclusion we have investigated a frustrated XY model with NNN interaction. The model can be experimentally realized in Josephson-junction arrays in a transverse magnetic field. Signatures of NNN Josephson couplings might already have been seen in specially designed setups.²⁵ The analysis presented here leads to the phase diagram shown in Fig. 5. For $0 < x < x_0$ the critical temperatures $T_c^{Z_2}$ and $T_c^{U(1)}(x)$ decrease with increasing x . For $x > x_0$, there is no sign of an Ising-like transition and the system behaves like the unfrustrated XY model. At $x \approx x_0$ in the low- T region there is a first-order phase transition between the low- and high- x phases. Finally for $x > x_0$ the array undergoes a sequence of two transitions. On raising the temperature, first the two sublattices become decoupled and then, at higher temperatures, each sublattice becomes disordered. The structure of the phase diagram remains the same if weak interaction with further neighbors is included

We thank H. Courtois and B. Pannetier for fruitful discussions. We acknowledge the financial support of INFM (PRA-QTMD) and the European Community (Contract No. FMRX-CT-97-0143). G.F. is grateful to A. Mastellone and J. Siewert for hospitality in Catania.

*Present address: Center for Polymer Studies, Boston University, 590 Commonwealth Avenue, Boston, MA 02215.

¹V. L. Berezinskii, Zh. Éksp. Teor. Fiz. **59**, 207 (1970) [Sov. Phys. JETP **32**, 493 (1971)]; J. M. Kosterlitz and D. J. Thouless, J. Phys. C **6**, 1181 (1973).

²P. Minnhagen, Rev. Mod. Phys. **59**, 1001 (1987).

³Proceedings of the NATO ARW on Coherence in Superconducting Networks, edited by J. E. Mooij and G. Schön [Physica B **152**, 1 (1988)]; Proceedings of the ICTP Workshop on Josephson Junction Arrays, edited by H. A. Cerdeira and S. R. Shenoy [Physica B **222**, 253 (1996)].

⁴D. J. Resnick *et al.*, Phys. Rev. Lett. **47**, 1542 (1981); H. S. J. van der Zant, H. A. Rijken, and J. E. Mooij, J. Low Temp. Phys. **82**, 67 (1991).

⁵Ch. Leemann *et al.*, Phys. Rev. Lett. **56**, 1291 (1986).

⁶T. J. Shaw *et al.*, Phys. Rev. Lett. **76**, 2551 (1996).

⁷W. Y. Shih and D. Stroud, Phys. Rev. B **30**, 6774 (1984); M. Y. Choi and S. Doniach, *ibid.* **31**, 4516 (1985).

⁸T. C. Halsey, Phys. Rev. B **31**, 5728 (1985).

⁹E. Granato and M. P. Nightingale, Phys. Rev. B **48**, 7438 (1993).

¹⁰S. Teitel and C. Jayaprakash, Phys. Rev. B **27**, 598 (1983); Phys. Rev. Lett. **51**, 1999 (1983).

¹¹J. Lee, J. M. Kosterlitz, and E. Granato, Phys. Rev. B **43**, 11 531

(1991).

¹²G. Ramirez-Santiago and J. V. José, Phys. Rev. B **49**, 9567 (1994).

¹³P. Olsson, Phys. Rev. Lett. **75**, 2758 (1995).

¹⁴G. Grest, Phys. Rev. B **39**, 9267 (1989).

¹⁵P. Olsson, Phys. Rev. B **55**, 3585 (1997).

¹⁶Models with competing interaction have been widely studied in the literature. See *Magnetic Systems with Competing Interactions*, edited by H. T. Diep (World Scientific, Singapore, 1994); P. Simon, J. Phys. A **30**, 2653 (1997); E. Branchina, H. Mohrbach, and J. Polonyi, Phys. Rev. D **60**, 045006 (1999).

¹⁷Josephson arrays with infinite range array were investigated in P. Chandra, L. B. Ioffe, and D. Sherrington, Phys. Rev. Lett. **75**, 713 (1995); H. R. Shea and M. Tinkham, *ibid.* **79**, 2324 (1997).

¹⁸C. L. Henley, Phys. Rev. Lett. **62**, 2056 (1989).

¹⁹M. Yosefin and E. Domany, Phys. Rev. B **32**, 1778 (1985).

²⁰M. Y. Choi and D. Stroud, Phys. Rev. B **32**, 5773 (1985).

²¹K. Binder, Z. Phys. B: Condens. Matter **43**, 119 (1981).

²²T. Ohta and D. Jasnow, Phys. Rev. B **20**, 139 (1979).

²³H. Weber and P. Minnhagen, Phys. Rev. B **37**, 5986 (1988).

²⁴P. Olsson, Phys. Rev. B **52**, 4526 (1995).

²⁵L. Glemot, B. Schmied, D. Achermann, P. Scheuzger, Ch. Leemann, and P. Martinoli (unpublished).